Biopolymer/ Glycopolypeptide Blended Scaffolds: Synthesis, Characterization and Cellular Interactions

Vinita Dhaware,[d,e] David Díaz Díaz*[b,c] and Sayam Sen Gupta* [a]

Abstract: Three-dimensional (3D) scaffolds formed from natural biopolymers gelatin and chitosan that are chemically modified by galactose have shown improved hepatocyte adhesion, spheroid geometry and functions of the hepatocytes. Galactose specifically binds to the hepatocytes *via* the asialoglycoprotein receptor (ASGPR) and an increase in galactose density further improves the hepatocyte proliferation and functions. In this work, we aimed to increase the galactose density within the biopolymeric scaffold by physically blending the biopolymers chitosan and gelatin with an amphiphlic β-galactose polypeptide (PPO-GP). PPO-GP, is a di-block copolymer with PPO and β-galactose polypeptide, exhibits lower critical solution temperature and is entrapped within the scaffold through hydrophobic interactions. The uniform distribution of PPO-GP within the scaffold was confirmed by fluorescence microscopy. SEM and mechanical testing of the hybrid scaffolds indicated pore size, inter connectivity and compression modulus similar to the scaffolds made from 100 % biopolymer. The presence of the PPO-GP on the surface of the scaffold was tested monitoring the interaction of an analogous mannose containing PPO-GP scaffold and the mannose binding lectin Con-A. In vitro cell culture experiments with HepG2 cells were performed on GLN-GP and CTS-GP and their cellular response was compared with GLN and CTS scaffolds for a period of seven days. Within three days of culture the Hep G2 cells formed multicellular spheroids on GLN-GP and CTS-GP more efficiently than on the GLN and CTS scaffolds. The multicellular spheroids were also found to infiltrate more in GLN-GP and CTS-GP scaffolds and able to maintain their round morphology as observed by live/dead and SEM imaging.

[a] Sayam Sen Gupta
Department of Chemical Sciences
Indian Institute of Science Education and Research-Kolkata
Mohanpur 741246, India
sayam.sengupta@iiserkol.ac.in
[b] David Diaz Diaz
Department of Natural Product Synthesis
Instituto de Productos Naturales y Agrobiología del CSIC
Avda. Astrofísico Francisco Sánchez 3, 38206 La Laguna, Tenerife (Spain)
d.diaz.diaz@ipna.csic.es
[c] David Diaz Diaz
Institute of Organic Chemistry
University of Regensburg, Universitätstrasse. 31, 93040 Regensburg (Germany)
David.Diaz@chemie.uni-regensburg.de
[d] Vinita Dhaware
Polymer Science Engineering Division
CSIR-National Chemical Laboratory
Dr. Homi Bhabha Road, Pune 411008, India
[e] Vinita Dhaware
Academy of Scientific and Innovative Research (AcSIR)
CSIR- Human Resource Development Centre, Campus Postal Staff College Area, Ghaziabad, 201002, Uttar Pradesh, India

Supporting information for this article is given via a link at the end of the document.

Introduction

Biopolymers such as gelatin and chitosan have gained wide attention as biomaterials in diverse tissue engineering applications due to their low cost, large-scale availability, biocompatibility and biodegradability.[1–3] These biopolymers mimic the natural extra-cellular matrices (ECM's) such as collagen, laminin and fibronectin whose physio-chemical properties control the spreading, migration, adhesion and proliferation of cells in tissue culture.[4] Although these biopolymer-based 3D-scaffolds have been shown to be excellent extracellular matrices for many cell types including fibroblasts, chondrocytes and mesenchymal stem cells; their functionalization by organic ligands have been shown to improve the adhesive. properties of these scaffolds towards cells. This enhanced efficacy is governed by a variety of factors that are characteristic of the scaffold surface. For example, in anchorage-dependent cells such as hepatocytes, which are mainly involved in carrying out liver functions, cell-substrate interactions affect cellular aggregation. Asialoglycoprotein receptors (ASGPR) on the surface of hepatocytes interact specifically with the galactose ligand and induce the formation of hepatocyte spheroids, which play a critical role in supporting their viability, proliferation and differentiation. Hence, incorporation of â-galactose residues onto 3D-scaffolds results in altered cellular behaviour and functions.[4–16] Galactosylated alginate has been shown to induce selective adhesion of hepatocytes, and formation and functional maintenance of spheroids.[5,13] In addition, galactosylated gelatin and chitosan sponges have been synthesized[5–11,14,16–18] and their efficacy in formation of hepatocyte aggregates was reported. The relationship between formation of larger hepatocyte aggregates and higher concentration of galactose ligand was studied by Ying *et al*. and Kobayashi *et al*.[19–21] One approach to introduce higher galactose density within the scaffold can be achieved through the introduction of galactose based glycopolymers rather than a monomeric ligand.[22] The interactions of monomeric carbohydrates with their corresponding receptor protein are weak but their specificity can be increased several-fold by displaying multiple copies of the carbohydrate on the ligand.[23]
We recently reported a strategy to introduce glycoprotein-mimetic glycopolypeptide onto silk fibroin films, which enhanced the surface activity of the naturally hydrophobic silk fibroin films and supported the growth of L929 cells.[24] However, introduction of galactose/glycopolymers onto the biopolymers requires multi-step chemical conjugation reactions. Such complex syntheses can be avoided if the monomeric or polymeric galactose can be physically incorporated into the natural biopolymer hydrogel. This is challenging since both monomeric and polymeric galactose molecules are hydrophilic and hence would leach out of the scaffold during cell culture experiments.

We hypothesized that such physical incorporation of glycopolypeptide would be possible with the synthesis of a galactose-based block-copolymer, in which one block would display LCST behaviour below physiological temperature. In such a scenario, the composite biopolymer-glycopolymer hydrogel formed at temperatures above its LCST would be resistant to the leaching due to the hydrophobic interaction between the PPO (above its LCST) and the hydrophobic domains of the biopolymer. Using this approach, we describe the synthesis of a composite hydrogel composed of the biopolymer gelatin/chitosan and an amphiphilic poly(propylene oxide)-β-galactose polypeptide (PPO-GP). PPO is a well-known FDA-approved polymer, with a lower critical solution temperature of 8 °C.[25] PPO-GP polymer was mixed with the biopolymers gelatin/chitosan and the cross-linker to form 3-D scaffolds by a freeze-drying technique. Scaffolds were thoroughly characterized to determine the pore size, distribution of the PPO-GP polymer in the scaffold, compression modulus and availability of the sugar moieties on the surface of the scaffold to interact with the cells. Human hepatoblastoma (HepG2) cells, which closely resemble the morphology and functioning of human hepatocytes were cultured within the scaffolds to study their potential of such structures to control cellular fate processes

.

Results and Discussion

Natural biopolymers such as chitosan and gelatin have been extensively used to fabricate 3D-hydrogels, which have shown promise as scaffolds for several soft tissue engineering applications including liver tissues.[1,5,7,11,14,17,18,27–29] For hepatocytes and hepatic cell lines that are present in liver tissues, the spheroid morphology is critical towards maintaining high liver-specific functions.[30] However, the trans-differentiation of hepatocytes into fibroblasts limits the culturing of hepatocytes and still remains a challenge.[31] The efficiency of spheroid formation is governed by many factors such as the pore size[13,32–34] of the scaffolds and availability of bioactive groups for cells to adhere on the material surfaces.[30] The ASGPRs present on hepatocytes and other hepatic cell lines bind specifically to the galactose moieties, thereby assisting these cells to achieve spheroidal morphology and maintain liver-specific functions.[4,9,14] Therefore, in order to improve the efficacy of these natural biopolymers (such as chitosan and gelatin) in aiding hepatic cell growth and proliferation in the 3D-scaffolds, several groups report the introduction of galactose moieties in the natural biopolymers, using chemical methods prior to the formation of scaffolds.[4,10,11,14,16,18,35–39] Since the binding of galactose to the receptors is a multivalent binding event, the density[15,40,41] and spatial orientation[42,43] of the galactose moieties are important parameters that influence cell morphology and function. For example, it has been shown that receptors bind efficiently to the tri-antennary molecules containing three galactose residues in comparison to the bi-antennary analogues containing two or one galactose residues.[40] Also, hepatocytes were reported to maintain their round morphology at lower galactose density if the galactose is spatially well oriented, to interact with cell surface receptors.[21] Based on the results reported earlier, we hypothesized that the formation of a hybrid scaffold using poly(propylene oxide)-β-galactose polypeptide (PPO-GP) in a biopolymer matrix such as gelatin or chitosan will significantly help the hepatic cells to maintain a spheroidal morphology. The PPO unit in PPO-GP is known to exhibit an LCST behaviour at 8 °C[25], hence a block polymer of PPO_{44}-GP_{12} should be amphiphilic in nature. The PPO segment will be held wthin it through hydrophobic interactions with the biopolymer matrix and the glycopolypeptide unit in the PPO-GP will serve as an multivalent binding site. This increases the efficacy of binding with hepatic cells via ASGPRs. This approach eliminates the need to perform demanding chemical conjugation of polymers into other biopolymers, as has been reported earlier.

Preparation of poly(propylene oxide)-β-galactose polypeptide (PPO-GP)

Amphiphilic PPO-GP was synthesized by our previous reported method.[26] Briefly, PPO-NH_2 was used as initiator for the ring-opening polymerization of β-D-galacto-L-lysine NCA in the presence of 1.0 equiv. of a proton sponge (M/I = 12) in dry DMF (ESI, Scheme 1). The resulting block copolymer was characterized by GPC and ^{1}H NMR (ESI, Figure S1 and S2). The M_n of the resulting polymer was calculated by integrating the anomeric proton at 5.69 ppm of galactose with the PPO (-CH-CH_3) protons at 1.07-1.11 ppm (ESI, Figure S2). The acetyl groups of the glycopolypeptide were removed completely using hydrazine monohydrate. The complete removal of acetyl groups was confirmed by the absence of acetyl protons in the ^{1}H NMR spectra of PPO-GP in DMSO (ESI, Figure S3). The deprotected PPO-GP formed a milky white or turbid solution in water at 25 °C, whereas a significant decrease in turbidity was observed when the solution was placed in the ice bath. This could be attributed to the presence of the PPO block in PPO-GP, which is well known to have an LCST at 8 °C.[25] Hence, at room temperature and above the PPO-GP block is amphiphilic, while at lower temperature the PPO-GP is more hydrophilic, resulting in decreased turbidity.

Formation and characterization of scaffolds with chitosan-PPO-GP and gelatin-PPO-GP hybrids

To construct the hybrid scaffolds with PPO-GP, both chitosan and gelatin were used as biopolymer. Hydrogels formed from chitosan and gelatin are widely used in biomedical applications, since both are derived from living organisms and are biocompatible, biodegradable, cause no inflammatory response to the host and have high water absorbing capacity.[44,45] Besides biocompatibility and biodegradability, the topology of the scaffold in nanometer and micrometer scale plays a very important role in controlling cell morphology and functions.[33,46] Scaffolds with voids of ca. 3 mm induced flat morphology of the cells, whereas voids greater than 70 μm promote three-dimensional aggregations due to the

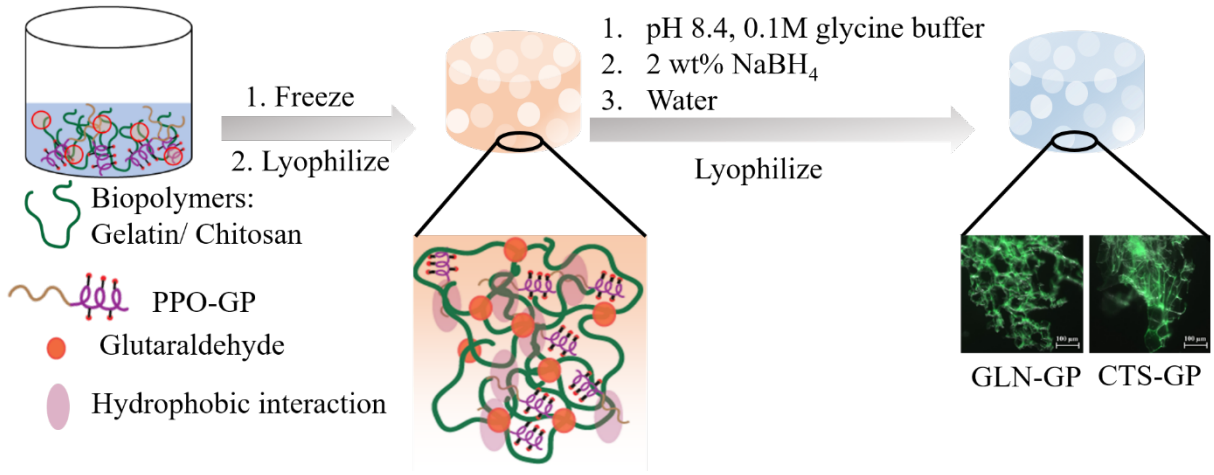

Figure 1. Schematic illustration of scaffold preparation

increased cell-cell contact.[13,32,47] In addition, to culture anchorage dependent cells such as hepatic cells the presence of cell surface receptor specific ligands is crucial. To introduce cell surface receptor specific ligands within the biopolymeric scaffolds, an amphiphilic PPO-GP containing multivalent binding site was blended with the biopolymer during scaffold formation. Both gelatin and chitosan are hydrophilic biopolymers that can readily cross link with glutaraldehyde and become converted into porous scaffolds after freeze drying.[48–50] Therefore, our scaffold preparation involved freezing of the biopolymer and glycopolypeptide PPO-GP mixture along with the cross linker glutaraldehyde, followed by lyophilization to achieve the desired porosities for 3D cell culture. For preparation of gelatin/PPO-GP blends, a solution of 30 mg/mL gelatin and 9 mg/mL PPO-GP was used (23 wt.% of PPO-GP in the composite). In the corresponding chitosan/PPO-GP blend, 10 mg/mL of chitosan and 3 mg/mL of PPO-GP was used (23 wt.% of PPO-GP in the composite). Since PPO-GP is hydrophilic at ice-cold temperatures, after the dissolution of gelatin by heating and chitosan using sonication, the biopolymer and PPO-GP mixture was placed in the ice bath
to attain uniform mixing (ESI, Figure S4). Finally, glutaraldehyde solution was added in a 1:1 proportion and the solutions were kept at -12 °C for gelatin/PPPO-GP and -40 °C for chitosan/PPO-GP, to induce scaffold formation. The PPO-GP entrapped gelatin-chitosan scaffolds were termed GLN-GP and CTS-GP respectively. The scaffolds formed from 100 % gelatin and chitosan (i.e. without any glycopolypeptide) that were used to perform control experiments were termed GLN and CTS. Since the residual glutaraldehyde left during scaffold formation is toxic to the cells, the porous scaffolds were subjected to a post-treatment to remove the excess glutaraldehyde and reduce the formed Schiff base, in turn imparting strength to the scaffolds[50] (Figure 1).

SEM images of the scaffolds revealed that the pore size in GLN and CTS as well as GLN-GP and CTS-GP scaffolds is from 20-120 µm with high porosity. All the scaffolds displayed heterogeneous porous structure with pore interconnectivity (Figure 2: A, B, D and E). Such interconnectivity can provide the cells with an ideal microenvironment during culture, thereby facilitating the migration of cells and growth factors, and enabling the supply of sufficient nutrients and gas exchange in deeper planes.[51] To ensure if the PPO-GP polymer was physically entrapped, 3D-scaffolds of the biopolymers were prepared using fluorescently labelled PPO-GP (ESI, Figure S5). Fluorescence microscopy images revealed that PPO-GP was uniformly distributed within the matrix on the pore walls of the biopolymer scaffolds (Figure 2: C and F). This fluorescent labelling also allowed us to study the amount of PPO-GP incorporated inside each scaffold. Therefore, to quantify the amount of PPO-GP entrapped within the hybrid scaffolds, we performed UV-vis measurements on the washings collected during scaffold synthesis using FL-GP and biopolymer. From the difference between the absorbance of the fluorescently labelled PPO-GP added and the absorbance of the combined washings, we were able to determine the amount of PPO-GP incorporated into each scaffold. The GLN-GP contained 4 wt.% of PPO-GP, whereas the corresponding CTS-GP contained 20 wt.% of biohydrogel. Considering that the aim of this study was to study the biological performance of HepG2 in these hybrid scaffolds, the stability of the PPO-GP towards leaching within the biopolymer scaffold during the culture period is extremely important. Hence, the FL-GP entrapped lyophilized scaffolds were soaked in PBS at 37 °C for seven days and the PBS was replaced with fresh PBS every day. The UV-vis spectra of the amount released as a function of time revealed that a further 2 % of PPO-GP was released from GLN-GP, whereas the CTS-GP scaffolds were found to be stable (ESI, Figure S6). Gelatin is composed of proline or hydroxyproline and glycine (more than 20% each) and the rest amino acids are 10% more and less. The amine in proline is a secondary amine and carboxyl is at the alpha position, whereas in chitosan has higher amounts of free primary amine groups. The PPO-GP interacts more efficiently with the free primary amine groups in chitosan as compared to the secondary amines of proline

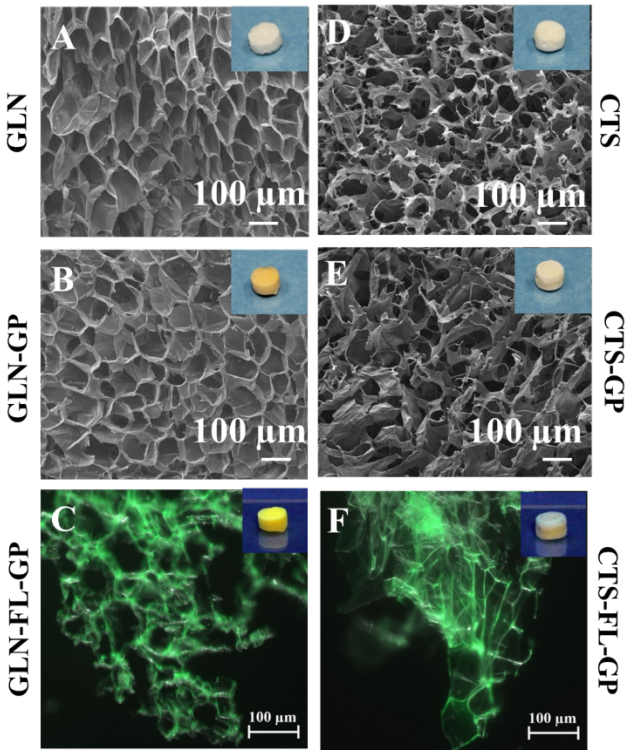

Figure 2. SEM Images (A-E); Fluorescence microscope image (C, F); Inset images: digital photo of the scaffolds in normal light (A-E); (C, F) under UV lamp

residues in gelatin resulting in differences in the stability of PPO-GP within the two scaffolds.

The mechanical properties of the scaffold play an important role in maintaining cell differentiation and proliferation.[52–54] The structural stability of the scaffolds is very important, to oppose the various stresses incurred during the cell culture period. The stiffness of the material on which the cells are lodged influences their morphology.[55] In order to model *in vivo* conditions we performed the mechanical test in the fully hydrated state of the scaffolds. The elastic modulus of a healthy liver is 1.5 kPa,[56] hence the stiffness of the scaffolds was evaluated by compressive modulus measurements. The compression modulus for the GLN and GLN-GP was 20 ± 3.3 kPa and 17 ± 0.8 kPa, respectively, whereas the CTS and CTS-GP showed 7 ± 3.5 kPa and 4 ± 1.3 kPa, respectively (Figure 3).

The high liver-specific functionality of the hepatocytes is maintained by their spheroid morphology and is affected by the affinity of the cells to interact with the material surfaces. Cho *et al*. and Griffith *et al*. have independently reported the importance of how the spatial distribution of galactose in the scaffold affects the morphology and function of hepatic cells.[42,43] The accessibility of galactose in spatial microdomains results in cell aggregation. To promote HepG2 adhesion, proliferation, spheroid morphology and penetration into deeper planes of the composite scaffold, the galactose moieties must be free to interact with the cells. Since PPO-GP is amphiphilic and stabilized in the biopolymer matrix through the hydrophobic PPO block, the hydrophilic galactose

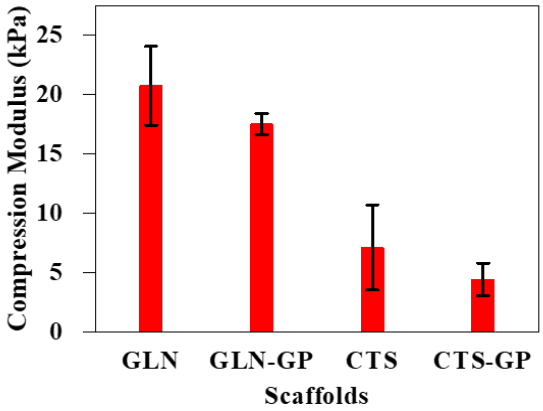

Figure 3. Compressive modulus of the scaffolds

block must be free to interact with the ASGPRs in HepG2. To ensure that the glycopolypeptide is available to interact with the cells in this composite scaffold, we synthesized a 3D scaffold with the homologous mannosylated PPO-mannose glycopolypeptide (PPO-Man). The mannose polypeptide was used because D-(+)-glucopyranoside and D-(+)-mannopyranoside residues with free 3-, 4-, and 6-hydroxyl groups are known to bind to the tetrameric protein Con A. Hence, if the carbohydrates within the composite scaffolds are exposed to the surface, they are expected to interact with the carbohydrate binding site of Con A.[24] The scaffolds formed with PPO-mannose (GLN-Man and CTS-Man) were treated with the fluorescently labelled Con A and then imaged using fluorescence microscopy (Figure 4). Both GLN-Man and CTS-Man showed aggregation of the Con A due to interaction with the mannose along the pore walls of the scaffold whereas such aggregations were absent in the GLN and CTS scaffolds (ESI, Figure S7). This observation suggests that the sugar moieties are free and bioactive. This further confirms that the entanglement of the PPO-GP polymer in the composite scaffold is mainly due to the hydrophobic character of the PPO chain.

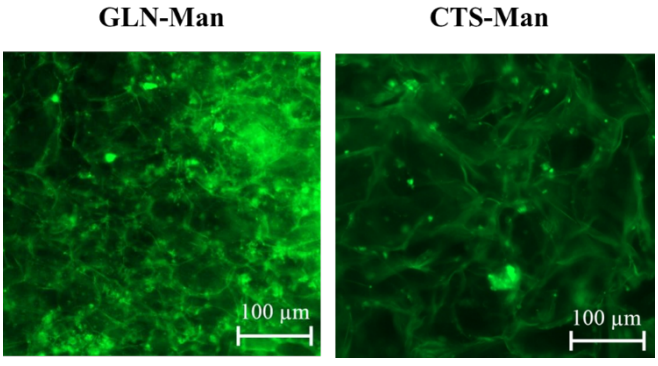

Figure 4. Fluorescence microscope images of scaffolds after interacting with FITC-Con A.

In vitro cell culture studies

Approximately 6 mm X 2 mm scaffolds were fabricated for the biological experiments. For CTS-GP, these scaffolds would contain 1 mg of CTS and 0.3 mg of PPO-GP. In the corresponding GLN-GP, 3 mg of GLN and 0.1 mg of PPO-GP were present. The biological performances of the composite scaffolds (CTS-GP and GLN-GP) and their pure biopolymer congeners (CTS and GLP) were studied by *in vitro* culturing of HepG2 cells for seven days. HepG2 proliferation on the CTS-GP and CTS were studied using MTT assay. Cell proliferation increased with time from day 1 to 7, irrespective of scaffold type, suggesting that all the scaffolds support the growth of the cells. There was increased cell viability on the CTS and CTS-GP scaffolds on day 7, in comparison to the GLN and GLN-GP (ESI, Figure S8**).**

Cellular infiltration is a key element for successful tissue regeneration and is dependent on the cell-matrix interaction, pore size and pore interconnectivity.[57] The sustained viability of the cells after infiltration within scaffolds is important to be able to apply these scaffolds for tissue engineering. We performed live/dead assays to assess the viability of the HepG2 cells and infiltration. Live cells detected by acridine orange exhibited green fluorescence, while propidium iodide marked the dead cells with a red fluorescence. The scaffolds at various time-points 3, 5 and7 days were stained with the live/dead reagents and their Z-stack image series were recorded using the confocal laser scanning microscope. The image series was then stacked to give a 3D representation of cell viability and infiltration within the scaffold. HepG2 cells were found to form aggregates on all the scaffolds. Interestingly, the aggregates on CTS-GP and GLN-GP composite scaffolds were found to be connected and larger at

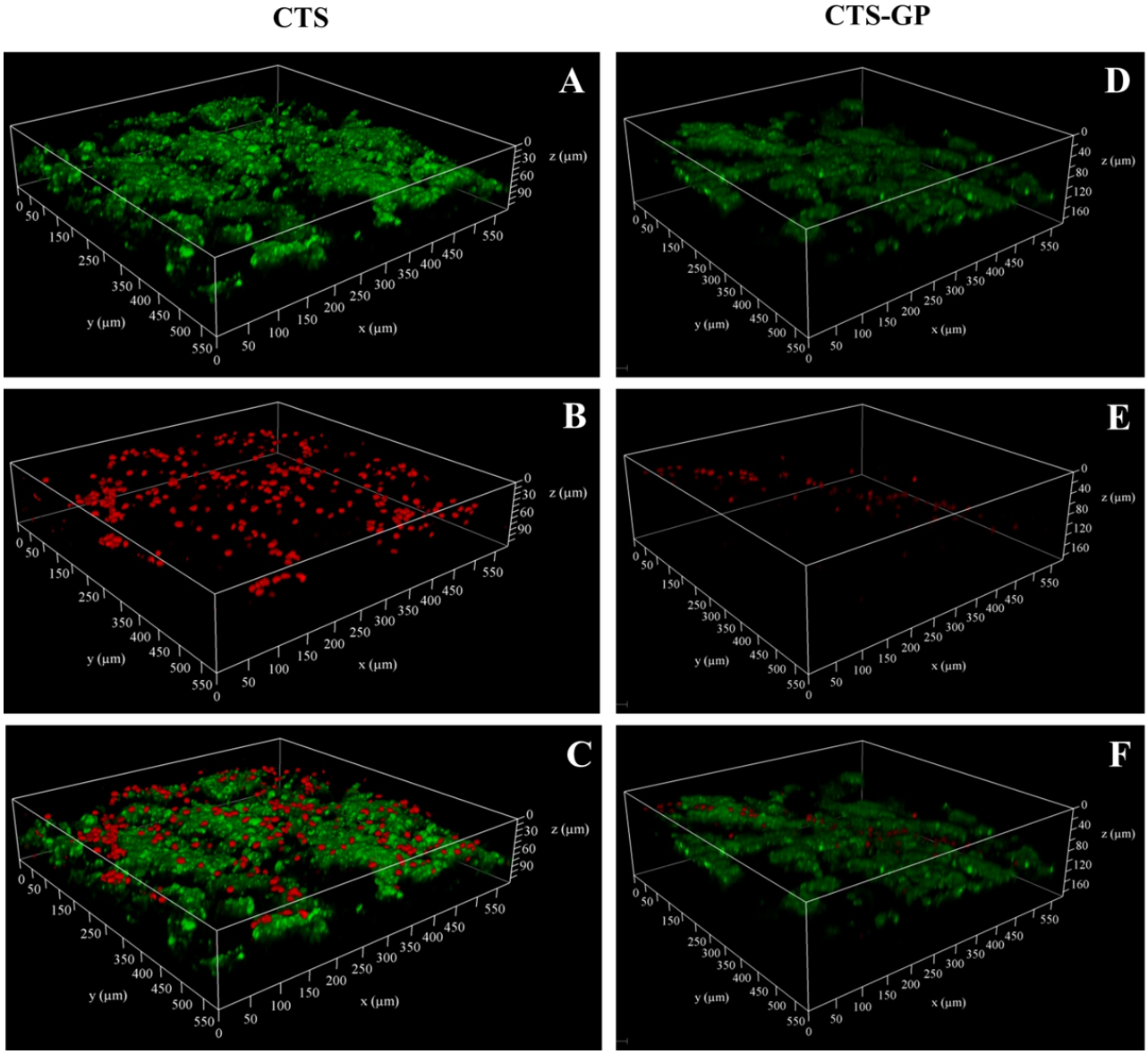

Figure 5**.** CLSM images of a live/dead assay of HepG2 cells, after 7 days of culture on CTS and CTS-GP recorded at 20X magnification to assess the viability of the cells after infiltration within the scaffolds. Figure (A & D) live, (B & E) dead, (C & F) merged image of live and dead

any given time point, compared to the CTS and GLN scaffolds where the aggregates were scattered. Another intriguing observation was that the number of dead cells within the aggregates on CTS and GLN scaffolds was higher than on the CTS-GP and GLN-GP (Figure 5, SI Figure S9, S10 and S11)

The Z-stack images revealed that after day 3 the cells covered a distance of approximately 45 µm on CTS, while for CTS-GP the migration observed was up to 50 µm. This trend continued to days 5 (ESI, Figure S9) and 7 (Figure 6), where migrations of 55 and 60 µm were observed in CTS scaffolds, whereas in CTS-GP the cells migrated up to 70 and 100 µm respectively in Z-direction. A similar increase in cell migration in Z-direction was observed for GLN-GP of 45, 110 to 160 µm, in comparison to the GLN scaffold. The latter showed migrations of 30, 70 and 110 µm on Day 3, 5 and 7 (ESI, Figure S10 and S12)

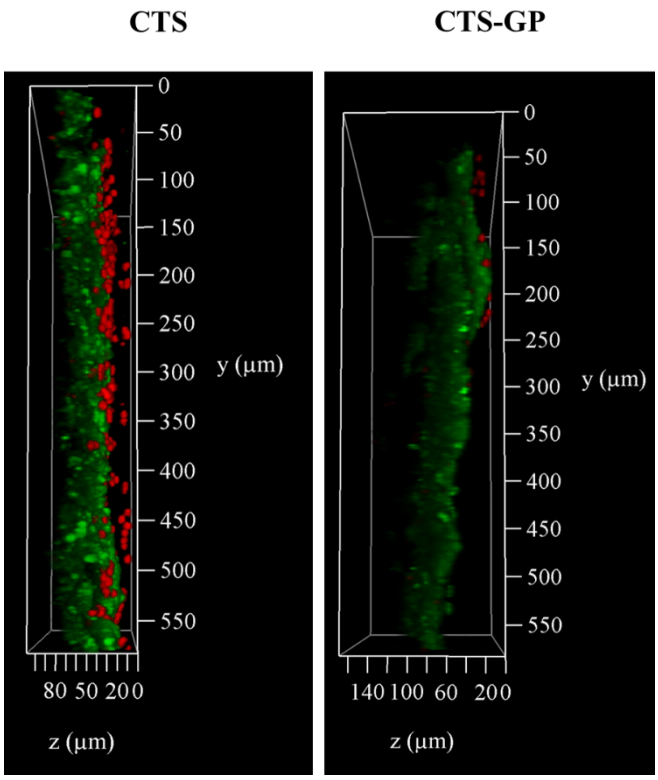

Figure 6: Z-stack of live/dead imaging of HepG2 cells cultured on CTS and CTS-GP scaffolds at day 7 to assess the depth of infiltration

Higher levels of liver-specific function are maintained by the spheroid cells resulting from the close packing of the cells, rather than by monolayer cells. The cytoskeleton plays an important role in cell migration, spreading and other cellular functions. Therefore, we examined the distribution of the actin skeleton of HepG2 by Alexa-488 staining. The compact arrangement of actin filaments in the aggregates was observed in the CTS-GP, whereas the actin filaments in cell aggregates on the CTS were spread out (Figure 7, day 7 and ESI, Figure S13 for days 3 and 5). Similar distribution of HepG2 cell actin filaments on GLN-GP and GLN scaffolds were observed (ESI, Figure S14 for days 3 and 5, Figure S15 for day 7). The compact arrangement indicates stronger cell-cell interaction is important to form the spheroid cell arrangement. Regulation of how cells adhere, proliferate and differentiate is strongly dependent on the cell-scaffold interaction.

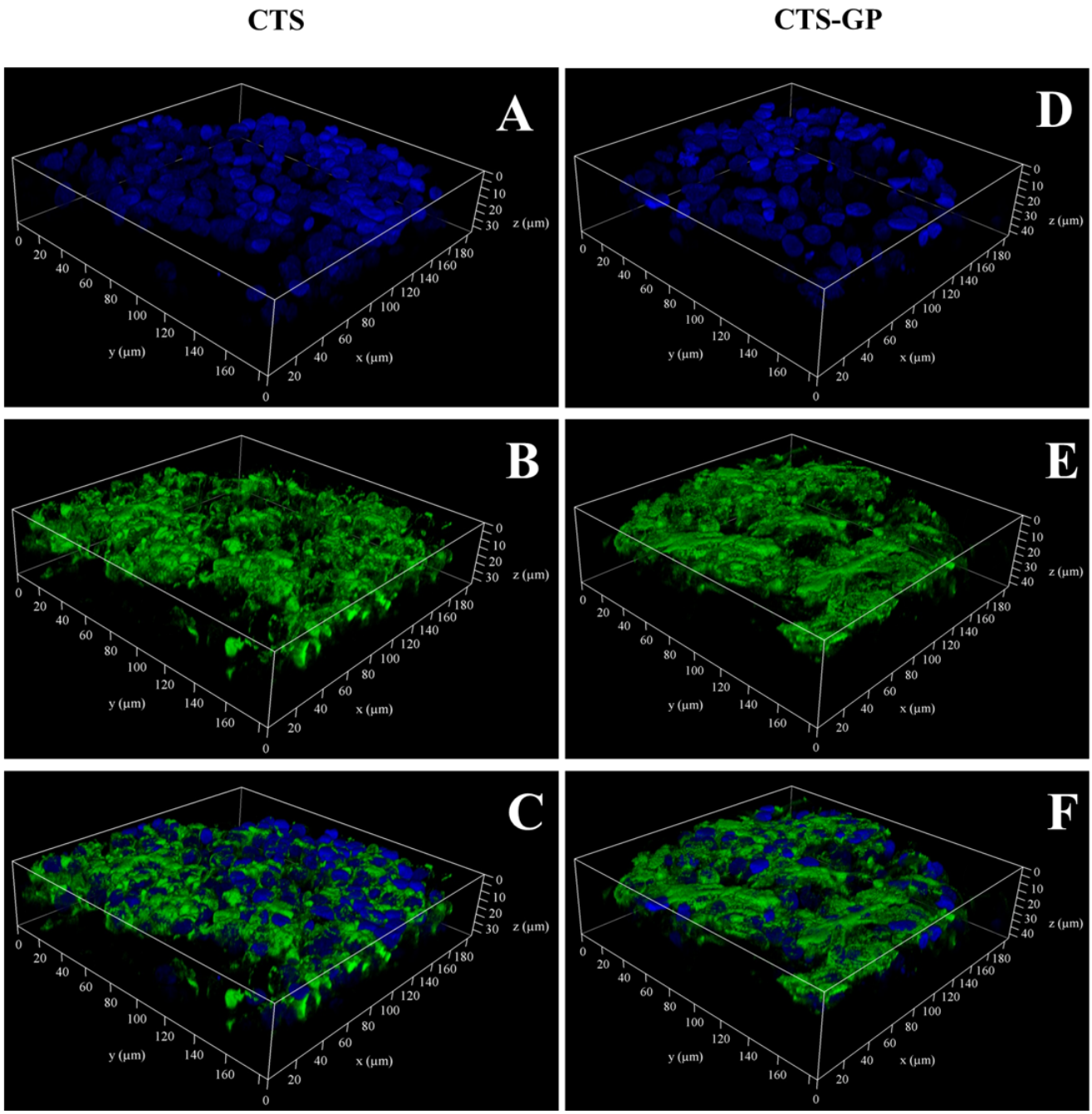

Figure 7. CLSM images of the compact arrangement of actin filaments of HepG2 on CTS and CTS-GP after 7 days of culture, recorded at 63X

In order to understand the cell-scaffold interaction, we examined the morphology of HepG2 cells cultured on day 7 using ESEM. The images revealed round cell shape and larger spheroids on CTS-GP scaffold, whereas the cells started losing their round morphology on the CTS (Figure 8). A similar form was seen on GLN-GP scaffolds in comparison to GLN scaffolds (ESI, Figure S16).

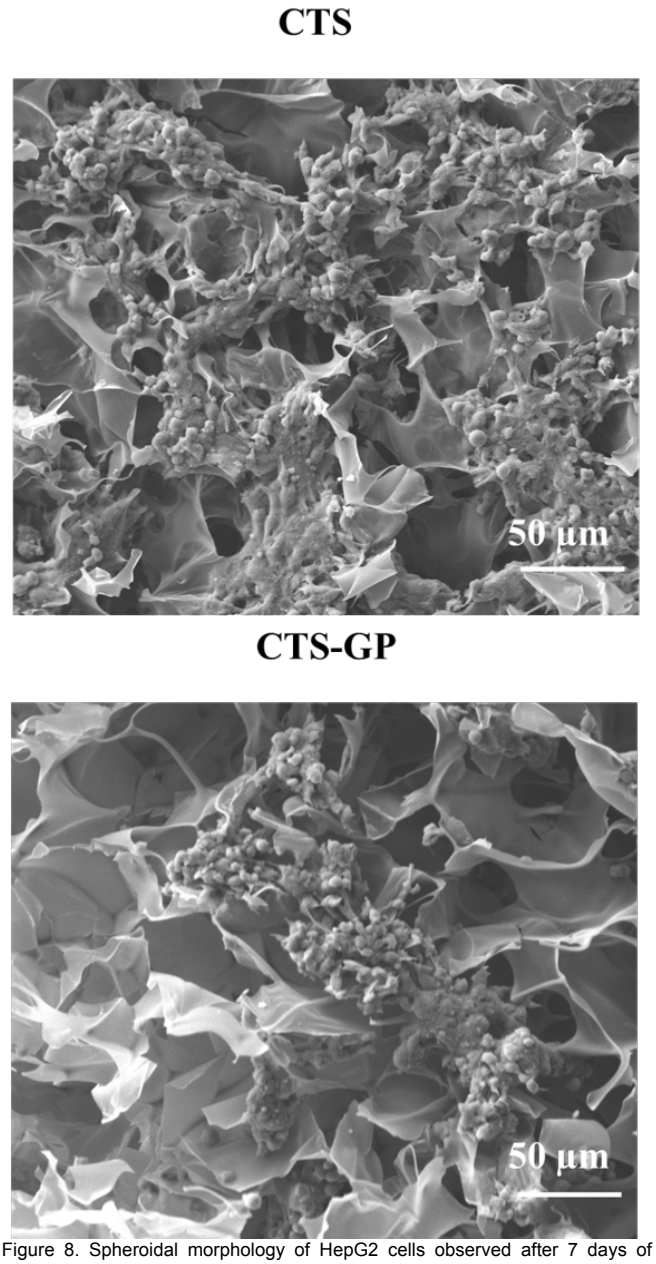

Figure 8. Spheroidal morphology of HepG2 cells observed after 7 days of culture on CTS and CTS-GP using SEM imaging.

Several studies have reported that chemical conjugation of scaffold materials with β-galactose residues improves hepatocyte attachment and aggregation.[4,9,58] In this study, a PPO-GP polymer was synthesized and physically entrapped in the biopolymer matrix via hydrophobic interactions. The composite scaffolds formed spheroids within 3 days of culture and more effectively than in control GLN and CTS scaffolds. Tamura et al. found that Hep G2 cell spheroids with diameters greater than 180 µm contained viable cells.[59] The difficulty in transport of oxygen and nutrients for spheroids larger than 200 µm resulted in the death of central cells of hepatocyte spheroids. The likely cause of cell death could be necrosis as reported by Torok *et.al*, Morieri *et.al*., Tamura *et.al*. and Gotoh *et.al* .[59-61] The results of the MTT cell viability assay indicated that it was similar in all four scaffolds.

The live/dead assay revealed that the spheroids formed in the GLN-GP and CTS-GP scaffolds were always larger than the GLN and CTS scaffolds at any given point in time. Dead cells within the spheroids were always located higher in the control scaffolds than the composite scaffolds. This indicates that the cells in spheroids undergo necrosis in the control scaffolds due to lack of oxygen and gas transport. Close packing of the cells is important in regulating the liver-specific functions. Actin staining revealed a more compact arrangement due to the close packing of the spheroids in hybrid scaffolds, which is essential in oxygen and gas transport. The SEM images of cell-cultured scaffolds revealed maintenance of the round morphology of the spheroids on the hybrid scaffolds, supporting the live/dead and actin stain results. The difference in the observations of the hybrid scaffolds could be attributed to the PPO-GP, which provides the cell surface ASGPRs on HepG2 with spatially oriented high galactose density. The stable porous structure and the presence of the β-galactose residues from PPO-GP Is primarily responsible for the enhanced activity

Conclusions

We formed 3-D porous scaffolds by physically blending amphiphilic poly(propylene oxide)-β-galactose polypeptide (PPO-GP) to increase the galactose densities within the scaffolds formed, using natural gelatin and chitosan biopolymers. The hybrid scaffolds were found to have interconnected heterogeneous pores and a compressive modulus comparable to the liver tissue. The sugar moieties on the scaffolds are free to interact with the cells was confirmed by studying the aggregation of the FITC-ConA on the CTS-GP and GLN-GP scaffolds The galactose moieties on the hybrid scaffolds were available for the cells to interact, thus promoting HepG2 adhesion and cell infiltration through the scaffold. The HepG2 cells formed larger spheroid aggregates and maintained their round morphology on the hybrid scaffold. Owing to the synergistic effect of the biopolymer and the PPO-GP polymer, the composite may be a promising substitute for use in liver tissue regeneration.

Experimental Section

Materials and Methods

Glyco-*N*-carboxyanhydride was prepared by using our previously published methodology.[26] $HAuCl_4$, triphosgene, propargyl amine, fluorescein-NHS, and fluorescein isothiocyanate (FITC)-labelled Con-A, gelatin from procrine skin (G2500), and chitosan (448877) were purchased from Sigma-Aldrich. DAPI, and Alexa-488 dyes were purchased from Invitrogen and used as received. All the other chemicals used were obtained from Merck, India. ^{1}H NMR spectra were obtained with a Bruker spectrometer (200.13 and 400.13 MHz) and reported relative signals according to the deuterated solvents used. Ultraviolet−visible (UV−vis) spectra were recorded on a Carry-300 UV−vis spectrometer using 1 cm quartz cuvettes at 25 °C. Fluorescence images were acquired using a Carl Zeiss epifluorescence microscope. Confocal images were obtained using the Leica confocal microscope.

Scaffold preparation

Hybrid gelatin-GP (GLN-GP) scaffold preparation. Gelatin (6 % w/v, 120 mg) along with PPO-GP (36 mg in 2 mL) was heated at 50 °C to dissolve gelatin. This mixture was placed in an ice bath to achieve homogenous solution, followed by the addition of glutaraldehyde (3 % w/v, 60 mL in 2 mL) solution. 0.1 mL of this mixture was then transferred to 96 well-plates and capped. The plates were placed in precooled methanol at -16 °C for 24 h. After 24 h, the scaffolds were transferred to sodium phosphate buffer (pH 8.4, 10 mM) containing 0.5 M of glycine (1 mL buffer per 0.1 mL of scaffold) for 8 h. The scaffolds were further treated with 1 mg/mL of sodium borohydride solution (1 mL solution/ 0.1 mL of scaffold) for another 18 h to reduce the Schiff bases changing the solution every 8 h. Finally, the scaffolds were washed with Milli-Q water overnight with two water changes. The control gelatin hydrogel (GLN) was prepared without PPO-GP polymer under similar conditions. The scaffolds were lyophilized for 8 h and kept under argon until further experiments.

Hybrid chitosan-GP (CTS-GP) scaffold preparation**.** The hybrid sponges were prepared by mixing the chitosan (2 wt.%, 20 mg) along with PPO-GP polymer (30 wt.%, 6 mg) in 1M acetic acid followed by sonication for 1 h to dissolve completely. After complete dissolution of chitosan the mixture was kept in an ice bath with intermittent vortexing to achieve a homogenous suspension. Glutaraldehyde (1.5 wt.%) was added in 1:1 ratio mixed thoroughly. Then, this solution (0.1 mL) was transferred to a 96-well polystyrene plate and frozen at -40 °C overnight. The frozen solutions were lyophilized affording a solid porous structure. Lyophilized scaffolds were transferred to 10 mM sodium phosphate buffer (pH 8.4) containing 0.5 M of glycine (1 mL buffer per 0.1 mL of scaffold) for 8 h. The scaffolds were further treated with 2 mg/mL of sodium borohydride solution (1 mL solution/0.1 mL) for 12 h and further in MilliQ water followed by lyophilization. The control chitosan (CTS) sponges were prepared without PPO-GP polymer under similar conditions. The lyophilized sponges were stored under argon until further use.

Estimation of the amount of PPO-GP incorporated into the scaffolds

PPO-Galactose polymer was labelled with fluorescein-*N*-hydoxysuccinimide by reacting the -NH2 end group with 5(6)-carboxyfluorescein NHS ester. The extent of labelling was found to be 20 % as determined by UV-vis studies. The hydrogels were prepared using the above-mentioned fluorescein-labelled PPO-GP (FL-GP). The aqueous washings during preparation of the scaffold were collected and the amount of polymer leached out during washings was estimated from the absorbance of the fluorescein attached to the PPO-GP. The difference between the amount of PPO-GP added during scaffold formation and the amount released during washings was used to estimate the amount of PPO-GP incorporated into the scaffold.

Stability of PPO-GP polymer in the hydrogel

The lyophilized scaffolds containing fluorescently labelled PPO-GP (FL-GP) were immersed in a known volume of PBS at 37 °C. After 24 hrs, the PBS was collected and replaced with fresh PBS buffer. The PBS extracts collected each day for a period of 7 days were used to estimate the leaching of the PPO-GP polymer from the scaffold using UV-vis spectroscopy (absorbance of fluorescently labelled PPO-GP).

Recognition of mannose residues by lectin Concanavalin A (Con A)

A 1 g/L solution of FITC−Con-A was prepared by dissolving FITC-Con-A in 0.1 M phosphate buffer (pH 7.2) containing 0.1 M NaCl, 0.1 mM $CaCl_2$ and 0.1 mM $MnCl_2$. Thin sections of scaffolds GLN, GLN-Man, CTS and CTS-Man were incubated in this FITC−Con-A solution at room temperature for 30 min. The thin sections were washed (3x) with 0.1 M phosphate buffer (containing 0.1 M NaCl, 0.1 mM $MnCl_2$ and 0.1 mM $CaCl_2$). Aggregation of FITC−Con-A on GLN-Man and CTS-Man was observed under a fluorescence microscope.

Mechanical measurements

Mechanical properties of gelatin hydrogels were measured using a strain-controlled rheometer from TA Instruments, RSA-III, equipped with a normal force transducer. All the samples were subjected to compressive strain at a rate of 0.05 mm/s. Mechanical properties of chitosan sponges were carried out using a TA-ARES controlled strain rheometer equipped with a normal force transducer. Compression stress–strain measurements were performed at a compression rate of 0.016 mm/s. All tests were performed using roughened parallel plates to prevent slippage of the sample during the test. All the measurements were done on wet scaffolds at room temperature (25 °C).

Scanning electron microscopy

Scanning electron microscopy (SEM) was performed using a FEI Quanta 200 3D environmental scanning electron microscope (ESEM). Cross sections of the freeze-dried samples were prepared by freeze fracture. A 24 nm gold film was sputtered (2 kV, 2 min) on the samples placed on carbon tape. Surface morphology, pore size, and pore interconnectivity were analysed using SEM. The pore sizes of the scaffolds were calculated using Image J software by choosing 25 random pores from three (n=3) scaffolds per group. The details are now incorporated in the experimental section.

Cell culture studies

HepG2 cells were procured from ATCC (American Type Culture Collection) and cultured in Minimum Essential Medium (MEM, Gibco, U.S.) supplemented with 10 % foetal bovine serum (FBS, Gibco, U.S.) at 37 °C, 5 % CO_2 in a humified incubator. Cells were passaged at 80 % confluency. To perform *in vitro* experiments the lyophilized scaffolds GLN, GLN-GP, CTS and CTS-GP were UV treated for 1 h and then, 20 µL of cell suspension containing 50,000 HepG2 cells was added onto the scaffolds and allowed to attach for 0.5 h. After 0.5 h the scaffolds were transferred into new wells and 1 mL of media was added. The scaffolds were transferred to new wells every alternate day and supplied with fresh media. The CTS and CTS-GP scaffolds were supplemented with 1 % antibiotic-antimycotic solution (Himedia, India).

Cytotoxicity assay**.** After specific incubation period, 400 µL of MTT solution (0.25 g/L) was added to the scaffolds and incubated for 4 h. After 4 h, 400 µL of DMSO was added and incubated at 37 °C for 0.5 h and the reading recorded at 550 nm.

Live/Dead assay**.** After specific incubation, the scaffolds were washed with PBS (× 3) and then incubated with serum-free media containing 5 % BSA for 1 h. Scaffolds were further incubated with 26.8 µM each of acridine orange and propidium iodide in serum-free media containing 5 % BSA for 30 min at 37 °C and washed with PBS (× 3). The scaffolds were imaged using a Leica SP8 spectral confocal laser scanning microscope with 20X objective.

Actin staining**.** After incubation, the scaffolds were washed with PBS (× 3) and then fixed with 4 % PFA at room temperature for 30 min followed by 10 min 0.1 % Triton-X treatment. Then, the scaffolds were washed with PBS (× 3), incubated with 5 % BSA followed by actin stain 1:100 dilutions for 1 h, DAPI for 10 min. The scaffolds were imaged using a Leica SP8 spectral confocal laser scanning microscope with 63X objective.

Scanning electron microscopy (SEM). The morphologies of HepG2 within the scaffolds were observed by SEM. The cell-seeded scaffolds were rinsed with PBS solution and fixed with 3 % glutaraldehyde in PBS at room temperature for 2 h and then washed with PBS three times each for 10 min. The scaffolds were dehydrated in graded ethanol solutions (20 %, 30 %, 50 %, 70 %, 80 %, 90 % ethanol) for 10 min each time, and finally

twice with pure ethanol for 10 min each. Samples were placed on carbon tape and 24 nm-sized gold films were sputtered (2 kV, 2 min) prior to imaging by FEI Quanta 200 3D environmental scanning electron microscope (ESEM).

Acknowledgements

V.D. is grateful for a fellowship from CSIR, New Delhi and thanks Farsaram Soni and Aniket Gudadhe for help in mechanical testing, and Dr. Anuya Nisal for valuable discussions. The authors thank Guido Vaughan Jones Carter (IPNA-CSIC) for manuscript proofreading. D.D.D. thanks the Deutsche Forschungsgemeinschaft (DFG) for the Heisenberg Professorship Award and the University of Regensburg for financial support.

Keywords: Spheroids • Adhesion • Cellular infiltration • Aggregates

[1] Y. Huang, S. Onyeri, M. Siewe, A. Moshfeghian, S. V. Madihally, *Biomaterials* **2005**, *26*, 7616.
[2] F. Croisier, C. Jérôme, *European Polymer Journal* **2013**, *49*, 780.
[3] H. Jiankang, L. Dichen, L. Yaxiong, Y. Bo, Z. Hanxiang, L. Qin, L. Bingheng, L. Yi, *Acta Biomaterialia* **2009**, *5*, 453.
[4] C. S. Cho, S. J. Seo, I. K. Park, S. H. Kim, T. H. Kim, T. Hoshiba, I. Harada, T. Akaike, *Biomaterials* **2006**, *27*, 576.
[5] F. Chen, M. Tian, D. M. Zhang, J. Y. Wang, Q. G. Wang, X. X. Yu, X. H. Zhang, C. X. Wan, *Materials Science & Engineering C-Materials for Biological Applications* **2012**, *32*, 310.
[6] Y. Qiu, Z. Mao, Y. Zhao, J. Zhang, Q. Guo, Z. Gou, C. Gao, *Macromolecular Research* **2012**, *20*, 283.
[7] Y. Shang, M. Tamai, R. Ishii, N. Nagaoka, Y. Yoshida, M. Ogasawara, J. Yang, Y. Tagawa, *Journal of Bioscience and Bioengineering* **2014**, *117*, 99.
[8] B. Wang, Q. Hu, T. Wan, F. Yang, L. Cui, S. Hu, B. Gong, M. Li, Q. C. Zheng, *International Journal of Polymer Science* **2016**, *2016*.
[9] T. W. Chung, J. Yang, T. Akaike, K. Y. Cho, J. W. Nah, S. Il Kim, C. S. Cho, *Biomaterials* **2002**, *23*, 2827.
[10] Z. Q. Feng, X. Chu, N. P. Huang, T. Wang, Y. Wang, X. Shi, Y. Ding, Z. Z. Gu, *Biomaterials* **2009**, *30*, 2753.
[11] E. Gevaert, T. Billiet, H. Declercq, P. Dubruel, R. Cornelissen, *Macromolecular Bioscience* **2014**, *14*, 419.
[12] A. Ghodsizadeh, H. Hosseinkhani, A. Piryaei, B. Pournasr, M. Najarasl, Y. Hiraoka, H. Baharvand, *Biotechnology Letters* **2014**, *36*, 1095.
[13] R. Glicklis, L. Shapiro, R. Agbaria, J. C. Merchuk, S. Cohen, *Biotechnology and Bioengineering* **2000**, *67*, 344.
[14] S. R. Hong, Y. M. Lee, T. Akaike, *Journal of Biomedical Materials Research - Part A* **2003**, *67*, 733.
[15] H. Ise, N. Sugihara, N. Negishi, T. Nikaido, T. Akaike, *Biochemical and Biophysical Research Communications* **2001**, *285*, 172.
[16] I.-K. Parka, J. Yangb, H.-J. Jeongc, H.-S. Bomd, T. A. I. Haradab, S.-I. Kima, C.-S. Cho, *Biomaterials* **2003**, *24*, 2331.
[17] J. Li, J. Pan, L. Zhang, Y. Yu, *Biomaterials* **2003**, *24*, 2317.
[18] J. Fan, Y. Shang, Y. Yuan, J. Yang, *Journal of Materials Science: Materials in Medicine* **2010**, *21*, 319.
[19] L. Ying, C. Yin, R. X. Zhuo, K. W. Leong, H. Q. Mao, E. T. Kang, K. G. Neoh, *Biomacromolecules* **2003**, *4*, 157.
[20] S. H. Kim, T. Hoshiba, T. Akaike, *Journal of Biomedical Materials Research - Part A* **2003**, *67*, 1351.
[21] A. Kobayashi, M. Goto, K. Kobayashi, T. Akaike, *Journal of Biomaterials Science, Polymer Edition* **1995**, *6*, 325.
[22] Y. Miura, Design and synthesis of well-defined glycopolymers for the control of biological functionalities. *Polymer Journal* **2012**, *44*, 679–689.
[23] D. Pati, A. Y. Shaikh, S. Das, P. K. Nareddy, M. J. Swamy, S. Hotha, S. Sen Gupta, *Biomacromolecules* **2012**, *13*, 1287.
[24] S. Das, D. Pati, N. Tiwari, A. Nisal, S. Sen Gupta, *Biomacromolecules* **2012**, *13*, 3695.
[25] S. S. Naik, J. G. Ray, D. A. Savin, *Langmuir* **2011**, *27*, 7231.
[26] S. Das, D. K. Sharma, S. Chakrabarty, A. Chowdhury, S. Sen Gupta, *Langmuir* **2015**, *31*, 3402.
[27] M. K. Aparnathi, J. S. Patel, P. D. Patel, *Biosci. Biotech. Res. Comm.* **2016**, *9*, 463.
[28] J. Yang, T. Woong Chung, M. Nagaoka, M. Goto, C. S. Cho, T. Akaike, *Biotechnology Letters* **2001**, *23*, 1385.
[29] M. Cheng, J. Deng, F. Yang, Y. Gong, N. Zhao, X. Zhang, *Biomaterials* **2003**, *24*, 2871.
[30] K. Kataoka, Y. Nagao, T. Nukui, I. Akiyama, K. Tsuru, S. Hayakawa, A. Osaka, N. H. Huh, *Biomaterials* **2005**, *26*, 2509.
[31] N. M. Meindl-Beinker, S. Dooley, In *Journal of Gastroenterology and Hepatology (Australia)*; 2008; Vol. 23.
[32] C. S. Ranucci, A. Kumar, S. P. Batra, P. V Moghe, *Biomaterials* **2000**, *21*, 783.
[33] F. Berthiaume, P. V Moghe, M. Toner, M. L. Yarmush, The FASEB journal : official publication of the Federation of American Societies for Experimental Biology **1996**, 10, 1471.
[34] J. Park, F. Berthiaume, M. Toner, M. L. Yarmush, A. W. Tilles, *Biotechnology and Bioengineering* **2005**, *90*, 632.
[35] M. Tian, B. Han, H. Tan, C. You, *Carbohydrate Polymers* **2014**, *112*, 502.
[36] Y. Du, S. mien Chia, R. Han, S. Chang, H. Tang, H. Yu, *Biomaterials* **2006**, *27*, 5669.
[37] Y. Wu, Z. Zhao, Y. Guan, Y. Zhang, *Acta Biomaterialia* **2014**, *10*, 1965.
[38] J. S. Desport, D. Mantione, M. Moreno, H. Sardón, M. J. Barandiaran, D. Mecerreyes, *Carbohydrate Research* **2016**, *432*, 50.
[39] G. Ashwell, J. Harford, *Annual Review of Biochemistry* **1982**, *51*, 531.
[40] C. Yin, L. Ying, P. C. Zhang, R. X. Zhuo, E. T. Kang, K. W. Leong, H. Q. Mao, *Journal of Biomedical Materials Research - Part A* **2003**, *67*, 1093.
[41] L. G. Griffith, S. Lopina, *Biomaterials* **1998**, *19*, 979.
[42] C. S. Cho, M. Goto, A. Kobayashi, K. Kobayashi, T. Akaike, *Journal of Biomaterials Science, Polymer Edition* **1996**, *7*, 1097.
[43] S. Kim, J. Kim, T. Akaike, **2003**, *553*, 433.
[44] P. P. Derivatives, J. Puiggal, *Gels* **2017**, *3*, 27.
[45] P. Jaipan, A. Nguyen, R. J. Narayan, *MRS Communications* **2017**, *7*, 416.
[46] C. S. Chen, M. Mrksich, S. Huang, G. M. Whitesides, D. E. Ingber, *Science* **1997**, *276*, 1425.
[47] B. A. C. Harley, H. Do Kim, M. H. Zaman, I. V. Yannas, D. A. Lauffenburger, L. J. Gibson, *Biophysical Journal* **2008**, *95*, 4013.
[48] B. Hoffmann, D. Seitz, A. Mencke, A. Kokott, G. Ziegler, *Journal of Materials Science: Materials in Medicine* **2009**, *20*, 1495.
[49] C. Y. Hsieh, S. P. Tsai, M. H. Ho, D. M. Wang, C. E. Liu, C. H. Hsieh, H. C. Tseng, H. J. Hsieh, **2006**.
[50] R. V Shevchenko, M. Eeman, B. Rowshanravan, I. U. Allan, I. N. Savina, M. Illsley, M. Salmon, S. L. James, S. V Mikhalovsky, S. E. James, *Acta Biomaterialia* **2014**, *10*, 3156.
[51] B. A. Blakeney, A. Tambralli, J. M. Anderson, A. Andukuri, D. J. Lim, D. R. Dean, H. W. Jun, *Biomaterials* **2011**, *32*, 1583.
[52] M. J. Buehler, Journal of the Mechanical Behavior of Biomedical Materials **2011**, 4, 125.
[53] R. G. Wells, The role of matrix stiffness in regulating cell behavior. *Hepatology* **2008**, *47*, 1394–1400.
[54] O. A. Lozoya, E. Wauthier, R. A. Turner, C. Barbier, G. D. Prestwich, F. Guilak, R. Superfine, S. R. Lubkin, L. M. Reid, *Biomaterials* **2011**, *32*, 7389.
[55] C. T. McKee, J. A. Last, P. Russell, C. J. Murphy, *Tissue Engineering Part B: Reviews* **2011**, *17*, 155.
[56] A. V. Janorkar, *ACS Symposium Series* **2010**, *1054*, 1.
[57] K. S. Vasanthan, A. Subramaniam, U. M. Krishnan, S. Sethuraman, *Journal of Materials Science: Materials in Medicine* **2015**, *26*.
[58] Y. Gotoh, Y. Ishizuka, T. Matsuura, S. Niimi, *Biomacromolecules* **2011**, *12*, 1532.

[59] T. Tamura, Y. Sakai, K. Nakazawa, *Journal of Materials Science: Materials in Medicine* **2008**, *19*, 2071.

[60] J. L. Moreira, P. M. Alves, J. G. Aunins, M. J. T. Corrondo, *Applied Microbiology and Biotechnology* **1994**, *41*, 203.

[61] É. Török, J. M. Pollok, P. X. Ma, P. M. Kaufmann, M. Dandri, J. Petersen, M. R. Burda, D. Kluth, F. Perner, X. Rogiers, *Cells Tissues Organs* **2001**, *169*, 34.